ZIBELINE INTERNATIONAL PUBLISHING

ISSN: 2616-4302 (Online)
CODEN: AMMCFL

RESEARCH ARTICLE

Acta Mechanica Malaysia (AMM)

DOI: http://doi.org/10.26480/amm.01.2020.11.15

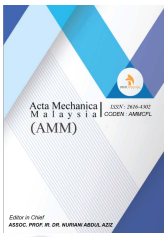

EFFECTS OF WELDING PARAMETERS, TIME INTERVAL AND PREHEATING ON RESIDUAL STRESS AND DISTORTION OF JOINING ST52 STIFFENER RING IN AN AISI 4130 TUBULAR SHELL

Alireza M. Haghighi*, Farhad S. Samani

Faculty of Mechanical Engineering, Shahid Bahonar University of Kerman, Kerman, Iran

**** Corresponding Author email:** alireza.m.haghighi@eng.uk.ac.ir; m.haghighi.alireza@gmail.com*

ARTICLE DETAILS

Article History:

Received 06 December 2019
Accepted 08 January 2020
Available online 17 February 2020

ABSTRACT

Stiffener rings and stringers are used commonly in offshore and aerospace structures. Welding the stiffener to the structure causes the appearance of residual stress and distortion that leads to short-term and long-term negative effects. Residual stress and distortion of welding have destructive effects such as deformation, brittle fracture, and fatigue of the welded structures. This paper aims to investigate the effects of preheating, time interval and welding parameters such as welding current and speed on residual stress and distortion of joining an ST52-3N (DIN 1.0570) T-shape stiffener ring to an AISI 4130 (DIN 1.7218) thin-walled tubular shell by eleven pairs of welding line in both sides of the ring by means of finite element method (FEM). Results in tangent (longitudinal), axial and radial directions have been compared and the best welding methods proposed. After the comparison of the results, simultaneous welding both sides of the ring with preheating presented as the best method with less distortion and residual stresses among the studied conditions. The correctness of the FEM confirmed by the validation of the results.

KEYWORDS

Arc Welding, Residual stress, Distortion, Simufact Welding, Finite Element Method.

1. INTRODUCTION

Thin-walled shells such as pipelines and tanks are used extensively in industries, especially offshore structures for transport and storage oil and chemical substances. They typically tolerate high constant or cyclic pressure of loading conditions which may be harmful and destructive and leads to deformation and fatigue (Chauhan and Syed, 2015). These types of shells should be stiffened against internal or external pressures. Internal and external rings or stringers are the affordable stiffeners for the tubular shells (Farkas et al., 2004; Gandhi et al., 2000). In some cases, geometrical limits are the reasons for using internal stiffeners (Rasti et al., 2014).

The welding process has a vast application in the manufacturing of simple to complex structures such as ships and bridges. Heating and cooling cycles during the welding process in the vicinity of stiffener-shell connections cause temperature differential between the welding heat zone and cold base metal (Cerik and Cho, 2013). This temperature gradient affects the thermal and physical properties of parts that occasion distortion and appearance of residual stresses in the tubular shell and stiffener ring with negative impacts on strength, assembly, and shape of the structure (Teng et al., 2001). This non-uniformly heating process leads to plastic strains that produce residual stresses. Subsequently, these stresses create internal forces that lead to distortion.

$$\varepsilon_x = \varepsilon_x^{'} + \varepsilon_x^{''} \tag{1}$$

$$\varepsilon_y = \varepsilon_y^{'} + \varepsilon_y^{''}$$
$$\varepsilon_z = \varepsilon_z^{'} + \varepsilon_z^{''}$$
$$\gamma_{xy} = \gamma_{xy}^{'} + \gamma_{xy}^{''}$$
$$\gamma_{yz} = \gamma_{yz}^{'} + \gamma_{yz}^{''}$$
$$\gamma_{xz} = \gamma_{xz}^{'} + \gamma_{xz}^{''}$$

Which ε_x, ε_y and ε_z are elastic and non-elastic strains in x, y and z directions respectively. γ_{xy} is shear strains in xy plane that $\gamma_{xy}^{'}$ is elastic strains and $\gamma_{xy}^{''}$ is non-elastic strains and so for other variables.

Heat stresses are

$$\varepsilon_x^{''} = \varepsilon_y^{''} = \varepsilon_z^{''} = \alpha.\Delta T$$
$$\gamma_{xy}^{''} = 0$$
$$\gamma_{yz}^{''} = 0$$
$$\gamma_{xz}^{''} = 0 \tag{2}$$

Quick Response Code	Access this article online	
	Website: www.actamechanicamalaysia.com	DOI: 10.26480/amm.01.2020.11.15

Cite The Article: Alireza M. Haghighi, Farhad S. Samani (2020). Effects Of Welding Parameters, Time Interval And Preheating On Residual Stress And Distortion Of Joining St52 Stiffener Ring In An Aisi 4130 Tubular Shell. *Acta Mechanica Malaysia , 4(1): 11-15.*

By using Hook's law

$$\varepsilon_x^{'} = \frac{1}{E}(\sigma_x - \upsilon(\sigma_y + \sigma_z))$$
$$\varepsilon_y^{'} = \frac{1}{E}(\sigma_y - \upsilon(\sigma_x + \sigma_z))$$
$$\varepsilon_z^{'} = \frac{1}{E}(\sigma_z - \upsilon(\sigma_x + \sigma_y)) \quad (3)$$
$$\gamma_{xy}^{'} = \frac{1}{G}\tau_{xy}$$
$$\gamma_{yz}^{'} = \frac{1}{G}\tau_{yz}$$
$$\gamma_{xz}^{'} = \frac{1}{G}\tau_{xz}$$

Which E is the elasticity modulus, ν is Poisson's ratio and G is shear modulus. A three-dimensional model creates six stress vectors of σ_x ‘ σ_y ‘σ_z‘ σ_{xy}‘ σ_{xz}‘ σ_{yz}.

There are some studies on the residual stress and distortion of welding the stiffener rings. A group researcher used the genetic algorithm and neural network to optimize the internal stiffener ring dimensions used in the pressure vessel made of high strength aluminum (Rasti et al., 2014). Some researchers analyzed two axisymmetric butt welds in stainless steel pipes with a wall thickness of 7.1 or 40.0 mm, by means of finite element method (FEM) (Yaghi et al., 2006). Maximum tensile stress for thin-walled pipe obtained near the inside surface, compressive stress near the outside surface and residual axial stresses influence by pipe diameter in the thin-walled pipe.

In other study, researchers presented the results of the static strength of axially loaded tubular T-joints with internal ring-stiffeners by means of numerical and experimental methods (Lee and Llewelyn-Parry, 1999). They found that failure is because of the formation of the plastic hinge from bending. A studied the tubular structure that stiffened internally with three rings under axial brace compression loadings and obtained that strength of the internally ring-stiffened joints is almost twice than the same unstiffened structure (Thandavamoorthy et al., 1999).

A group researcher presented three-dimensional finite element simulation, including pipe diameter effects in welding the steel pipe and discussed the differences (Lee and Chang, 2008). A studied numerically and experimentally, residual stress and temperature transient in joint of the 3D tubular structure (Barsoum, 2007). In other study, researchers investigated the residual stress of joining two tubular structures made of structural steel S355J2H to find a relation between material microstructure and residual stress. Distortion of large structures studied by many researchers (Hemmesi et al., 2016). A group researcher developed an elastic finite element method to predict the distortion of welding large structures (Deng et al., 2007). Some researcher proposed a local/global approach to predict welding distortion of large structures (Duan et al., 2007).

Welding parameters such as current and speed are very effective on the quality of welding and the magnitude of residual stresses. Welding current control, the quality and penetration depth of the process. Welding speed has a direct influence on the costs because it controls the timing of the process. Other effective parameters such as preheating, and time intervals are very effective in welding quality and distribution of residual stresses and distortion. Preheating and time interval are simple methods to reduce the plastic deformations by making thermal balance that leads to less residual stresses and distortion. The purpose of this paper is to study the effects of welding parameters on residual stress and distortion of joining the ST52-3N (DIN 1.0570) T-shape stiffener ring in an AISI 4130 (DIN 1.7218) thin-walled tubular shell by considering preheating and time intervals. Finally, by comparison of different methods and situations, the best welding methods are suggested.

2. PROBLEM EXPLANATION, INNOVATIONS & AIMS OF PAPER

An AISI 4130 (DIN 1.7218) thin-walled tubular shell stiffened by an ST52-3N (DIN 1.0570) T-shape ring with eleven pairs of weld lines of ER70S-6 on both sides of the ring and the effects of welding parameters such as welding current and speed on residual stresses and deformations of the structure have been investigated in different conditions by considering preheating and the time intervals between welding each side of the ring. Figure 1 shows the clipped 3D model of a thin-walled tubular shell stiffened by a T-shape ring.

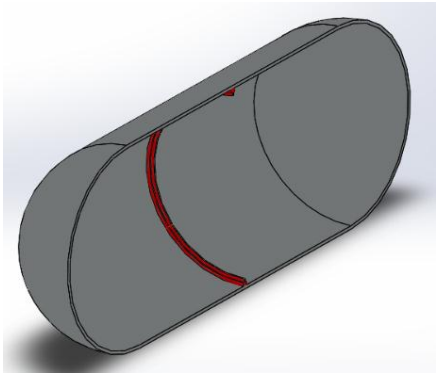

Figure 1: Clipped model of the thin-walled tubular shell stiffened by T-shape ring (specified by red color)

ST52-3N (DIN 1.0570) is general structural carbon steel with good weldability and impact resistance which melting point is 1538℃ and tensile strength is 490 MPa and density of 7855 kg/m^3. AISI 4130 (DIN 1.7218) is a common material in offshore structures with the density of 7801 kg/m^3, yield strength is 450 MPa and the melting point is 1480℃. ER70S-6 has a high level of Deoxidizers welding of steels that is suitable for welding of steels with moderate amounts of scale or rust is applied (ER70S-6, 2019). The density of this material is 7870 kg/m^3 and the melting point of 1538℃.

3. RESEARCH METHOD AND ASSUMPTIONS

The FE simulation has been carried by means of Simufact Welding software. First, the FEM by means of Simufact Welding has been validated. Other researcher investigated on residual stress of butt welding of two ASTM 36 carbon steel plates simulated by means of ANSYS software (Dragi and Ivana, 2009). They used element birth and death technique for the weld line and compared the residual stress results with the experimental method. Figure 2 shows the model and position of the weld line of this study. In Stamenković's study, welding current assumed 180 A, the voltage was 24 V and the welding speed of 5 mm/s (Dragi and Ivana, 2009).

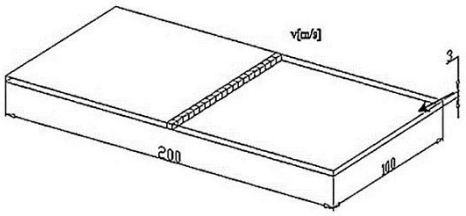

Figure 2: Model of study on residual stress of butt welding of ASTM 36 plates (Dragi and Ivana, 2009)

This process simulated in Simufact Welding software to compare and validate the results. Figure 3 shows the comparison of the results of Simufact Welding software with Stamenković's study (Dragi and Ivana, 2009). The validation shows high accuracy and the low error rate of the software results. Moreover, near the weld line, the results of Simufact Welding are more accurate than the FEM of the article. So, it validated as an accurate method with reliable results. In the following sections, the model is developed and the residual stresses and distortion of joining the stiffener ring to the thin-walled tubular shell are estimated.

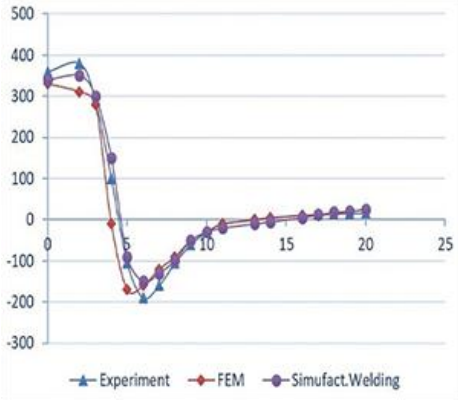

Figure 3: Validation of the results of the Simufact Welding software with the Stamenković's study (Dragi and Ivana, 2009)

The model designed and meshed in order to import as an input of the software (Li et al., 2019). The tubular shell is 300 mm radios and 700 mm length with 2 mm thickness. Stiffener ring placed in the middle of the shell and welded with eleven pairs of weld lines of 10 mm length and 5 mm leg length. The structure meshed by 38222 tetrahedral elements and 13636 nodes. Figure 4 shows the meshed structure and position of weld lines.

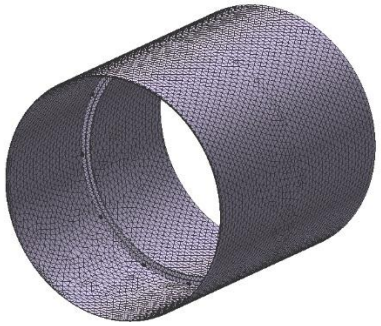

Figure 4: Meshed model for FEM and position of weld lines

The Goldak double ellipsoid model has been used as the heat source. Figure 5 shows the Goldak's ellipsoid model.

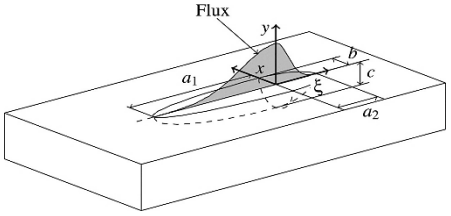

Figure 5: Heat source Goldak's double ellipsoid model (Lorin et al., 2014)

Table 1 shows the dimensions of Goldak's model of the problem.

Table 1: Dimensions' of Goldak's ellipsoid model

a_1	a_2	b	c
3.9	14.3	6	2

Which a_2 is the front length, a_1 is rear length, b is width and c is depth of the heat source.

Heat distribution in front and rear of ellipsoid are:

$$q_f(x,y,z) = \frac{6\sqrt{3} f_f Q}{bca_2\pi\sqrt{\pi}} e^{(-3x^2/b^2)} e^{(-3y^2/c^2)} e^{(-3z^2/a_2^2)} \quad (4)$$

$$q_r(x,y,z) = \frac{6\sqrt{3} f_r Q}{bca_1\pi\sqrt{\pi}} e^{(-3x^2/b^2)} e^{(-3y^2/c^2)} e^{(-3z^2/a_1^2)} \quad (5)$$

Parameters f_f and f_r are factors of temperature distribution that $f_f + f_r = 2$ calculate as:

$$f_f = \frac{2}{1+\frac{a_1}{a_2}} \quad (6)$$

$$f_r = \frac{2}{1+\frac{a_2}{a_1}} \quad (7)$$

Inserted energy distributes as Gaussian mode in any direction through the ellipsoid. Figure 6 shows the peak temperature of welding process of the model in welding simultaneously which raise to 1538°C.

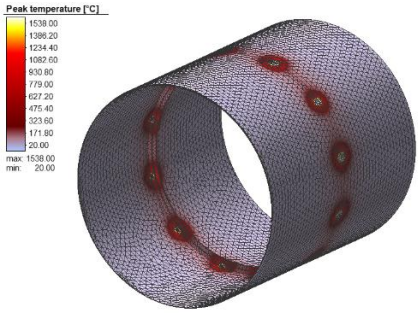

Figure 6: Peak temperature of simultaneous welding both sides of the ring

4. RESULTS AND DISCUSSION

Welding has been simulated on the model in different conditions of welding and effective parameters. The primer current is 210 A, voltage is 25 V, and the speed is 9 cm/min and 0.9 of heat efficiency. The software automatically increased the mesh density beside the weld line simultaneous with the welding process in order to decrease the error rate in heat-affected zone. Welding in the same direction has less residual stress and distortion than welding in opposite directions. Also, separation of the weld line to smaller weld lines reduces these phenomena (Callister and Wiliam, 2000). So, both sides of the ring have been welded in the same direction and separated into eleven weld lines. The welding process has been simulated in different situations by considering welding parameters, preheating and time intervals. Table 2 shows the results of FEM in different conditions. Current has been changed 15% from default measure in some cases and speed has been changed subsequently in a way to keep the net energy per length constant. Time intervals assumed as the time that takes the weld lines of one side of the ring to cool down and then the other side has been welded. In this model, the time interval considered 200 seconds. Residual stresses in main radial directions in different conditions exploited as shown in table 2.

Table 2: Maximum and minimum stresses of considered model in main radial directions and maximum of effective stress.

I [A]	S [Cm/min]	t_i [s]	H [°C]	Tangent (Longitudinal) stress [MPa]		Axial stress [MPa]		Radial stress [MPa]		Effective stress [MPa]
				Max	Min	Max	Min	Max	Min	Max
210	9	–	–	195	-142	420	13	63	-52	364
210	9	200	–	173	-140	390	-2	65	-51	375
210	9	–	150	160	-125	357	10	58	-42	288
241	9	–	–	185	-141	422	9	63	-58	342
178.5	7.6	–	–	199	-149	425	-10	63	-47	345
210	9	200	150	162	-145	380	4	64	-52	315

Where I is current, S is speed, V is voltage, t_i is the interval speed and H is preheating.

According to the results of stresses in main radial directions, the minimum values of tangent stress refer to simultaneous welding with preheating (Max: 162 MPa, Min: -145 MPa), and welding with time interval and preheating (Max: 160 MPa, Min: -125 MPa). Simultaneous welding with preheating (Max: 357 MPa) has the least axial stress. Simultaneous welding (Max: 420 MPa) and simultaneous welding by increasing and decreasing 15% to the current (Max: ~423 MPa) present the highest values of axial residual stress. The contour of the residual stress of simultaneous welding with preheating shown in Figure 7.

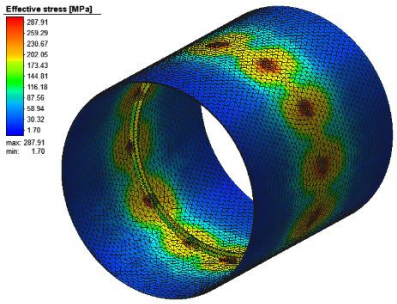

Figure 7: Distribution contour of the effective stress of simultaneous welding with preheating

Maximum distortion of the process in main radial directions and total distortion of the model in considered conditions shown in table 3.

Table 3: Effects of welding and effective parameters on distortion of the model

I [A]	S [cm/Min]	t_i [s]	H [°C]	Max.tangent distortion [mm]	Max axial distortion [mm]	Max.radial distortion [mm]	Max.total distortion [mm]
210	9	–	–	0.59	0.46	0.72	0.77
210	9	200	–	0.35	0.37	0.49	0.61
210	9	–	150	1.06	0.59	1.12	0.57
241.5	10.3	–	–	0.64	0.42	0.72	1.28
178.5	7.6	–	–	0.64	0.46	0.73	0.69
210	9	200	150	0.80	0.58	0.82	0.38

The least tangent (longitudinal) distortion refers to welding simultaneously (Max: 0.59 mm), and welding with the time interval (Max: 0.35 mm). In the axial direction, welding with the time interval (Max: 0.37 mm), and welding by increasing 15% to the current have less distortion (Max: 0.42 mm). Almost, welding by increasing and decreasing 15% to current have almost constant results in all conditions. In the radial direction, distortion results are almost constant in most of the conditions but welding with the time interval (Max: 0.49) has the least distortion among them.

Overall, the total distortion of welding by increasing 15% to the current has the most (Max: 1.28 mm), and simultaneous welding with preheating (Max: 0.57 mm) and welding with time interval and preheating (Max: 0.38 mm) have the least values among considered cases. Distribution contour of total distortion of welding with preheating shown in Figure 8.

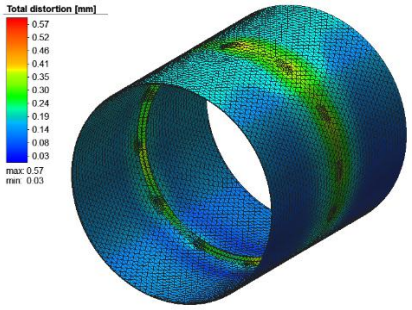

Figure 8: Distribution contour of total distortion of simultaneous welding with preheating

Figure 10 shows the effects of preheating and Figure 11 shows the effects of time interval on effective stress (von Mises stress) of the model which have been exploited from the line of nodes cross two weld lines as shown in Figure 9.

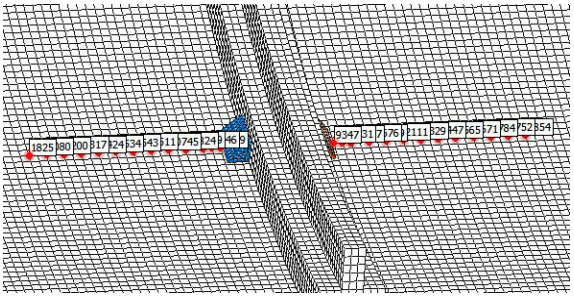

Figure 9: Line of nodes (red dots) considered to exploit plots

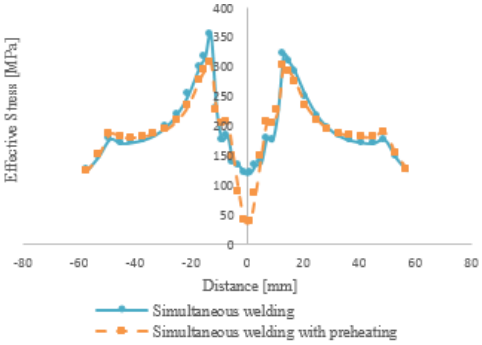

Figure 10: Effects of preheating on effective stress of welding simultaneously.

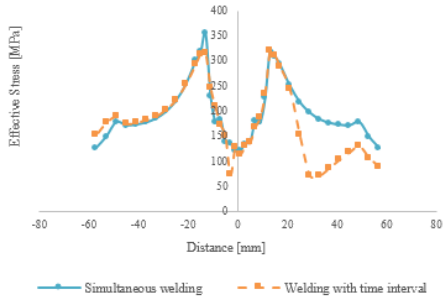

Figure 11: Effects of time interval on effective stress of the model

Current at a specific speed is the most effective parameter in the welding process that controls the fusion rate of the electrode and main parts and has many effects on residual stress and distortion of the model. Figure 12 shows the effects of changing welding current on effective stress.

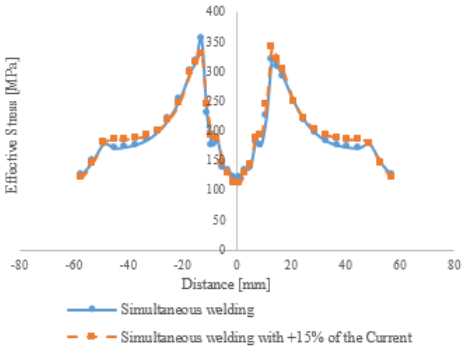

Figure 12: Effects of welding current on effective stress of welding simultaneously

5. CONCLUDING REMARKS

Based on FE analysis of welding the ST52-3N (DIN 1.0570) T-shape stiffener ring in an AISI 4130 (DIN 1.7218) thin-walled tubular shell by eleven pairs of weld lines on both sides of the ring, preheating by making a heat balance and decreasing cooling slope of the parts, reduces plastic deformation and residual stresses. By considering the residual stresses and distortion of different welding conditions in all main radial directions, simultaneous welding with preheating is the best method of welding an ST52-3N (DIN 1.0570) T-shape stiffener ring in an AISI 4130 (DIN 1.7218) thin-walled tubular shell among residual stresses and distortion of considered conditions. Effective stress and total distortion of welding conditions are shown in Figure 13 and Figure 14, respectively.

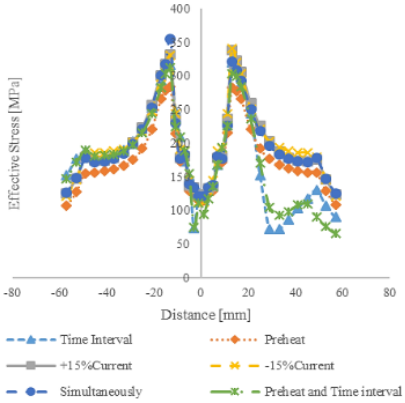

Figure 13: Comparison of effective stresses in considered conditions

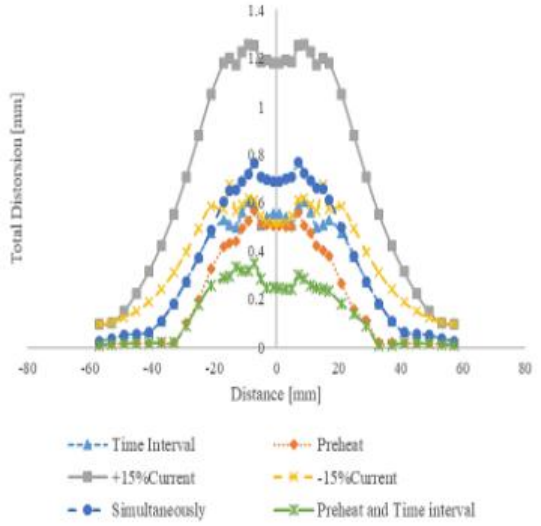

Figure 14: Comparison of total distortion in considered conditions

CONFLICTS OF INTEREST

The authors declare no conflict of interest.

REFERENCES

Barsoum, Z., 2007. Residual Stress Prediction and Relaxation in Welded Tubular Joint. Welding in the World, 51 (1-2), Pp. 23-30.

Callister, William Jr. Materials science and engineering, an introduction. New York: Wiley.

Cerik, B., Cho, S., 2013. Numerical investigation on the ultimate strength of stiffened cylindrical shells considering residual stresses and shakedown. Journal of Marine Science and Technology, 18 (4), pp. 524-534.

Chauhan, V.S., Syed, S.Q., 2015. Numerical Stress Analysis of Uniform and Stiffened Hydraulic Cylinder. International Journal of Scientific Engineering and Research (IJSER), https://www.ijser.in/archives/v3i4/IJSER1580.pdf, 3 (4), 55 – 59.

Deng, D., Murakawa, H., Liang, W., 2007. Numerical simulation of welding distortion in large structures. Computer Methods in Applied Mechanics and Engineering, 196 (45-48), pp. 4613-4627.

Dragi, S., Ivana, V., 2009. Finite element analysis of residual stress in butt welding two similar plates. Scientific Technical Review, 59 (1), pp. 57-60.

Duan, Y., Vincent, Y., Boitout, F., Leblond, J., Bergheau, J., 2007. Prediction of welding residual distortions of large structures using a local/global approach. Journal of Mechanical Science and Technology, 21 (10), pp. 1700-1706.

ER70S-6 - WeldWire", WeldWire, 2019. [Online]. Available: http://www.weldwire.net/weld_products/ww70s-6/. [Accessed: 04-Mar- 2019].

Farkas, J., Jármai, K., Virág, Z., 2004. Optimum Design of a Belt-Conveyor Bridge Constructed as a Welded Ring-Stiffened Cylindrical Shell. Welding in the World, 48 (1-2), pp. 37-41.

Gandhi, P., Raghava, G., Murthy, D., 2000. Fatigue Behavior of Internally Ring-Stiffened Welded Steel Tubular Joints. Journal of Structural Engineering, 126 (7), pp. 809-815. Available: 10.1061/(asce)0733-9445(2000)126:7(809).

Hemmesi, K., Farajian, M., Siegele, D., 2016. Numerical and experimental description of the welding residual stress field in tubular joints for fatigue assessment. Welding in the World, 60 (4), Pp. 741-748.

Lee, C., Chang, K., 2007. Three-dimensional finite element simulation of residual stresses in circumferential welds of steel pipe including pipe diameter effects. Materials Science and Engineering: A, 487 (1-2), Pp. 210-218.

Lee, M., Llewelyn-Parry, A., 1999. Strength of ring-stiffened tubular T-joints in offshore structures. Journal of Constructional Steel Research, 51 (3), Pp. 239-264.

Li, X., Xue, X., Zhang, L., Wang, X., Wang, H., 2019. Experiment and Finite Element Analysis on the Ultimate Strength of Ring-Stiffened Tube-Gusset Joints. International Journal of Steel Structures, 19 (5), Pp. 1534-1542. 2019.

Lorin, S., Cromvik, C., Edelvik, F., Lindkvist, L., Söderberg, R., 2014. Variation Simulation of Welded Assemblies Using a Thermo-Elastic Finite Element Model. Journal of Computing and Information Science in Engineering, 14 (3), Pp. 031003. Available: 10.1115/1.4027346.

Rasti, A., Sattarifar, I., Salehi, M., Karimnia, V., 2014. Stress analysis of welded joints in internal stiffener rings in an aluminum cylinder. Proceedings of the Institution of Mechanical Engineers, Part L: Journal of Materials: Design and Applications, 230 (1), pp. 121-130.

Teng, T., Fung, C., Chang, P., Yang, W., 2001. Analysis of residual stresses and distortions in T-joint fillet welds. International Journal of Pressure Vessels and Piping, 78 (8), pp. 523-538.

Thandavamoorthy, T., Rao, A., Santhakumar, A., 1999. Behavior of Internally Ring-Stiffened Joints of Offshore Platforms. Journal of Structural Engineering, 125 (11), pp. 1348-1352.

Yaghi, A., Hyde, T., Becker, A., Sun, W., Williams, J., 2006. Residual stress simulation in thin and thick-walled stainless-steel pipe welds including pipe diameter effects. International Journal of Pressure Vessels and Piping, 83 (11-12), Pp. 864-874.